

# Polypropylene mesh for hernia repair with controllable cell adhesion/de-adhesion properties

Sonia Lanzalaco,<sup>a,b,§</sup> Luis Javier Del Valle,<sup>a,b</sup> Pau Turon,<sup>c</sup> Christine Weis,<sup>c</sup>

Francesc Estrany,<sup>a,b</sup> Carlos Alemán,<sup>a,b</sup> Elaine Armelin<sup>a,b,§</sup>

<sup>a</sup> *Departament d'Enginyeria Química, EEBE, Universitat Politècnica de Catalunya, C/*

*Eduard Maristany, 10-14, Ed. I.2, 08019, Barcelona, Spain.*

<sup>b</sup> *Barcelona Research Center for Multiscale Science and Engineering, Universitat*

*Politécnica de Catalunya, C/ Eduard Maristany, 10-14, Ed. I.5, 08019, Barcelona, Spain.*

<sup>c</sup> *Research and Development. B. Braun Surgical, S.A. Carretera de Terrassa 121, 08191*

*Rubí (Barcelona), Spain.*

<sup>§</sup> Corresponding authors: [sonia.lanzalaco@upc.edu](mailto:sonia.lanzalaco@upc.edu) and [elaine.armelin@upc.edu](mailto:elaine.armelin@upc.edu)

## 2. Experimental section

### 2.3. Physical-chemical characterization

The graft yield (GY, in mg/cm<sup>2</sup>) of the iPP-g-PNIPAAm samples was evaluated from the weight increases after the graft polymerization. The grafting amount of PNIPAAm on the treated PP mesh was calculated as follows (Eq. S1):

$$GY (mg/cm^2) = \frac{w_f - w_0}{A} \quad (S1)$$

where  $w_f$  and  $w_0$  represent the weight of the mesh after and before grafting, respectively, while  $A$  is the area of iPP mesh.

The equilibrated swelling ratio (ESR, in %) of the PNIPAAm hydrogel covalently bonded to iPP mesh was obtained after the immersion of iPP-g-PNIPAAm samples in 10 mL of milli-Q water for 24 hours at 25 °C. After removal from vessel and elimination of the water in excess, the ESR was measured using the following Eq. (S2):

$$ESR (\%) = \frac{w_s - w_d}{w_d} * 100 \quad (S2)$$

where  $w_s$  and  $w_d$  are the weights of swollen (24h) and dry gel, respectively. The accuracy of the measurements was 3%. All measurements were performed in triplicate.

FTIR spectra were recorded on a Jasco 4000 FTIR spectrometer, equipped with a diamond ATR device (Golden Gate, Bruker). The absorption was measured in a wavenumber range from 4000 to 600 cm<sup>-1</sup>, after 64 accumulation scans at 8 cm<sup>-1</sup> of resolution, and after baseline correction.

X-Ray photoelectron spectroscopy (XPS) analyses were used for the detection of chemical species of PNIPAAm gel grafted during 1 and 2 h supported on aluminium substrate. The assays were performed on a SPECS system equipped with an Al anode XR50 source operating at 150 mW and a Phoibos MCD-9 detector. The pressure in the analysis chamber was always below 10<sup>-7</sup> Pa. The pass energy of the hemispherical analyser was set at 25 eV and the energy step was set at 0.1 eV. Data processing was performed with the Casa XPS program (Casa Software Ltd., UK).

## Supporting Information

Field Emission Scanning electron microscopy (FE-SEM) were carried out using a Focused Ion Beam Zeiss Neon40 scanning electron microscope equipped with an energy dispersive X-ray analysis (EDX) spectroscopy system and operating at 5 kV. The SEM was used to examine the surface morphology of pristine Optilene® Mesh LP fibers and fibers covered by PNIPAAm crosslinked with MBA hydrogel (Optilene® Mesh LP-*g*-PNIPAAm) and the effect of the crosslinker concentration and reaction time. The meshes were mounted on a double-side adhesive carbon disc and sputter-coated with a thin layer of carbon to prevent sample charging problems. In order to observe the internal microstructure of the porous hydrogel, in this step, the samples were dried by freeze drying (after the graft reaction) and the cross-section of mesh fibers were observed under cryo-fracture conditions. Samples used in optical microscopy (Linkam microscope) were previously dried under vacuum for 24h at room temperature.

Atomic force microscopy (AFM) images were taken with a Molecular Imaging PicoSPM and a NanoScope IV controller, under ambient conditions. The AFM tapping mode was operated at constant deflection. The row scanning frequency was set to 1 Hz. AFM measurements were performed on various parts of Optilene® Mesh LP-*g*-PNIPAAm, which provided reproducible images. The scan window sizes used were 10×10 μm<sup>2</sup>. The statistical application of the NanoScope Analysis software was used to determine the root mean square roughness ( $R_q$ ), which is the average height deviation taken from the mean data plane.

Confocal imaging was performed using an Axio Observer Z1 fluorescence microscope (Carl Zeiss), confocal laser scanning microscope with a 10x objectives. Morphology studies were performed with ImageJ software. Before confocal imaging, the cells were fixed and stained for nucleus and F-actin on day 1. After 24h cells were washed with PBS and fixed with 2.5 % paraformaldehyde in PBS for 40 min at room temperature. Later on, samples were washed 3 times 5 min each with PBS and permeabilized with 0.05% (w/v) triton X-100 in PBS for 20 min under agitation. After this, unspecific sites were blocked with a solution containing 1% bovine serum albumin, 22.52 mg/mL glycine and Tween-20 0.1 % in PBS for 30 min. F-actin filaments were stained with phalloidin atto-488 (Stock solution 10 nmol/500 uL methanol) used with a 1/50 dilution in PBS for 60 min at room temperature under agitation. Again, samples were washed 3 times 5 min

each with PBS. Finally, cell nucleus was stained with bis-benzimide H33258 (Stock solution 2 mM) employed at 1/100 dilution in PBS during 30 min under soft constant agitation and mounted on the glass slides. Samples were protected from light and kept at 4 °C before use.

#### **2.4. Biological studies**

Cellular assays were performed using epithelial (MCF-7) and fibroblast (COS-1) cells. Such cell lines were selected due to their well-known rapid growth. Cells were cultured in Dulbecco's Modified Eagle Medium (DMEM) high glucose supplemented with 10% FBS, penicillin (100 units/mL), and streptomycin (100 µg/mL). The cultures were maintained in a humidified incubator with an atmosphere of 5% CO<sub>2</sub> and 95% O<sub>2</sub> at 37 °C. Culture media were changed every two days. When the cells reached 80-90% confluence, they were detached using 2 mL of trypsin (0.25% trypsin/EDTA) for 5 min at 37°C. Finally, cells were re-suspended in 5 mL of fresh medium and their concentration was determined by counting with a Neubauer camera using 0.4% trypan blue as a vital dye.

Untreated and plasma treated Optilene® Mesh LP as well as Optilene® Mesh LP-*g*-PNIPAAm samples with an area of 1 × 1 cm<sup>2</sup> were fixed in stainless steel substrates and were placed in polystyrene plates of 24 wells and sterilized using UV irradiation for 15 min in a laminar flux cabinet. We had to adhere the mesh to metal surface due to its low density and problems of mesh floating on the culture media. Therefore, our "control" is the stainless steel substrates alone, without the PP mesh, instead of polystyrene wells. Controls were simultaneously performed by culturing cells on the surface of steel; in the same conditions than *iPP-g*-PNIPAAm. For adhesion and cytotoxicity assays 2 × 10<sup>4</sup> and 5 × 10<sup>4</sup> of cells respectively, were deposited on the surface sample of each well. Then, attachment of cells to the film surface was promoted by incubating under culture conditions for 30 min. Finally, 2 mL of the culture medium were added to each well. After 24 h, all cells in the well were quantified to evaluate its adhesion to the materials, after 7 days in incubation the cells in the well were again quantified to evaluate the cytotoxicity of the materials, whereas cellular viability was determined by quantifying exclusively the cells attached to films.

Cellular viability was evaluated by the colorimetric MTT [3-(4, 5-dimethylthiazol-2-yl)-2, 5-diphenyltetrazolium bromide] assay, which determines the cell viability. This assay measures the ability of the mitochondrial dehydrogenase enzyme of viable cells to cleave the tetrazolium rings of the MTT and form formazan crystals, which are impermeable to cell membranes and, therefore, are accumulated in healthy cells. This process is detected by a colour change: the characteristic pale yellow of MTT transforms into the dark-blue of formazan crystals. Specifically, 50  $\mu$ L of MTT solution (5 mg/mL in PBS) were added to each well. After 3 h of incubation, samples were washed twice with PBS and stored in clean wells. In order to dissolve formazan crystals, 1 mL of DMSO/methanol/water (70/20/10 % v/v) was added. Finally, the absorbance was measured in a plate reader at 570 nm. The viability results, derived from the average of four replicates (n= 4) for each independent experiment, were normalized to the control, for relative percentages.

## 2.5. Statistical analysis

Each sample was evaluated using four replicates, results being averaged and graphically represented. The statistical analysis was performed by one-way ANOVA test to compare the means of all groups. The t-Test was applied to determine a statistically significant difference between different groups. The tests were performed with a confidence level of 95% (p <0.05).

## 3. Results and discussion

### 3.2. Influence of the grafting time on the composition and swelling properties of iPP-g-PNIPAAm platforms

**Table S1.** O/C, N/C, N/O ratios and atomic concentration of C1s, O 1s and N 1s obtained by XPS high resolution spectra for Optilene® Mesh LP-g-PNIPAAm samples.

Sample code	Element	Atomic conc. (%)	O\C ratio	N\C ratio	N\O ratio
1h	C 1s	78.09	0.20	0.08	0.43
	O 1s	15.31			
	N 1s	6.59			
2h	C 1s	77.49	0.18	0.11	0.63
	O 1s	13.78			
	N 1s	8.73			

**Table S2.** Atomic concentration of functional groups obtained from O 1s peak deconvolution for Optilene® Mesh LP-*g*-PNIPAAm samples with 1h and 2h of grafting reaction.

Sample code	Functional group	Binding energy (eV)	Atomic conc. (%)
1h	O 1s (Al-O)	530.80	23,71
	O 1s (O-H, N-C=O))	531.92	70,81
	O 1s (C-O-C)	533.42	5,48
2h	O 1s (Al-O)	530.63	22,12
	O 1s (O-H, N-C=O))	531.42	69,86
	O 1s (C-O-C)	533.17	8,02

### 3.3. Effect of grafting time for the deposition of PNIPAAm on the 2D-geometry of the monofilament polypropylene mesh

Focusing the attention on the mesh fibers and, in order to understand the distribution of the gel on them, additional atomic force microscopic analysis (AFM) was carried out. Chemical grafting reaction between iPP and NIPAAm monomer starts from functional groups created on the polypropylene fibers. AFM images of Optilene® Mesh LP plasma functionalized and iPP-*g*-PNIPAAm copolymers grafted during 1 and 2 h are reported in Figure S1. Modification in the roughness, as is shown in the 2D-height, 2D-amplitude and 3D-topographic AFM images of the Optilene® Mesh LP fibers were observed (Figures S1 a-c). The appearance of new chains ascribable to PNIPAAm hydrogel, after 1 h of grafting, was observed as well as their increase when the grafting time was doubled (2 h). The oxygen-plasma treated sample presents a surface roughness, expressed in terms of  $R_q$ , of  $49.4 \pm 5.6$  nm, while a remarkable increase of  $R_q$  was observed in the presence of the gel, being  $78.4 \pm 2.4$  nm and  $170.0 \pm 6.6$  nm for samples grafted during 1 and 2h, respectively.

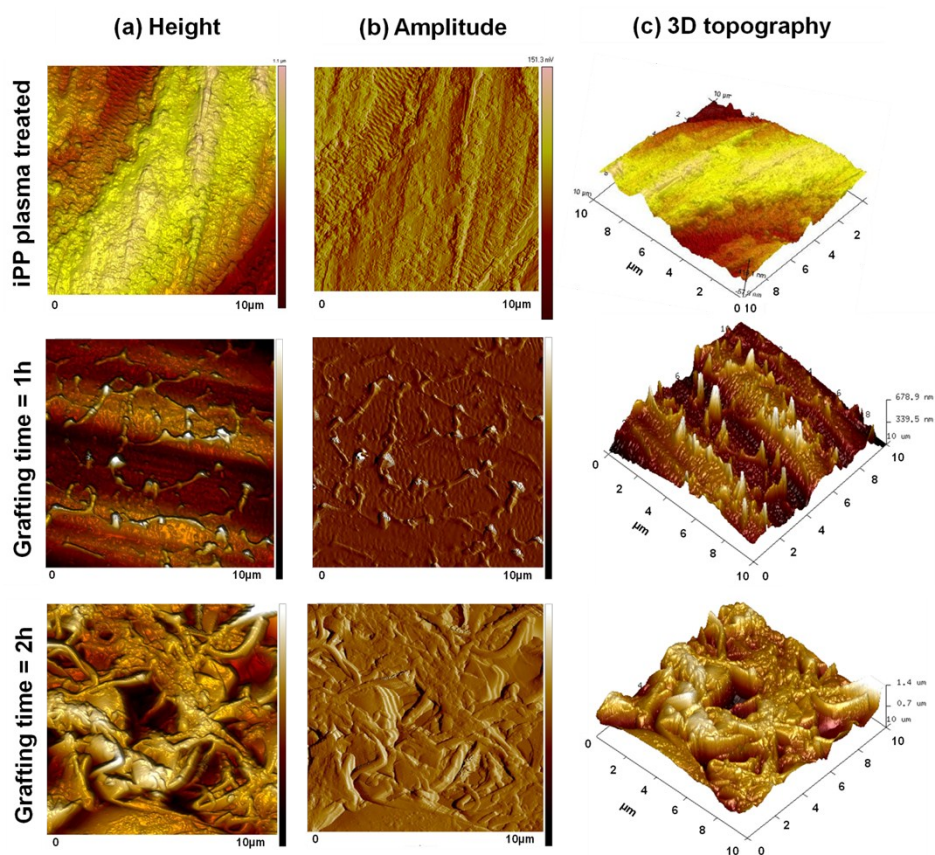


Figure S1. Sets of high resolution topography images of plasma treated Optilene® Mesh LP and iPP-g-PNIPAAm obtained during 1h and 2 h of grafting (scale: 10×10 μm<sup>2</sup>). AFM images: (a) height, where dark and brighter areas represent the depressions and the protrusions, respectively, on the 3D surface; (b) amplitude showing the deflection generated by cantilever tip; and (c) 3D topographic images.

### 3.5. Morphology of cells in the iPP-g-PNIPAAm mesh platforms

In the Figure S2, it is possible to identify some COS-1 cells trapped on the iPP-g-PNIPAAm fibres (grafting time of 2 h and MBA content of 1mM), that corroborates the confocal laser scanning microscopy images showed in the Figure 11 (main text).

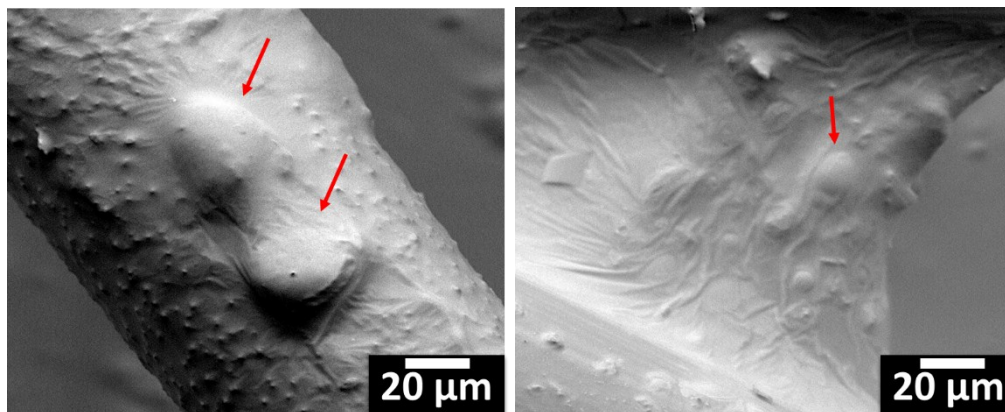


Figure S2. SEM micrographs taken from iPP-g-PNIPAAm fibre (a) and PNIPAAm hydrogel deposited among fibres (b), after grafting time of 1h and cell culture with COS-1 cells, after 7 days of cells proliferation. Red arrows indicate the regions where some COS-1 cells are detected.

### References

- 1 C. Minogianni, K. G. Gatos and C. Galiotis, *Appl. Spectrosc.*, 2005, **59**, 1141–1147.
- 2 J. Martin, M. Ponçot, J. M. Hiver, P. Bourson and A. Dahoun, *J. Raman Spectrosc.*, 2013, **44**, 776–784.
- 3 T. Sundell, H. Fagerholm and H. Crozier, *Polymer (Guildf.)*, 1996, **37**, 3227–3231.
- 4 Y. C. Tyan, J. Der Liao, Y. Te Wu and R. Klauser, *J. Biomater. Appl.*, 2002, **17**, 153–178.
- 5 S. Gorgieva, M. Modic, B. Dovgan, M. Kaisersberger-Vincek and V. Kokol, *Plasma Process. Polym.*, 2015, **12**, 237–251.
- 6 R. M. Khafagy, *J. Polym. Sci. Part B Polym. Phys.*, 2006, **44**, 2173–2182.
- 7 D. E. Gen, K. A. Prokhorov, G. Y. Nikolaeva, E. A. Sagitova, P. P. Pashinin, B. F. Shklyaruk and E. M. Antipov, *Laser Phys.*, 2011, **21**, 125–129.
- 8 M. Arruebarrena de Baez, P. J. Hendra and M. Judkins, *Spectrochim. Acta Part A*, 1995, **51**, 2117–2124.
- 9 G. Masetti, F. Cabassi and G. Zerbi, *Polymer (Guildf.)*, 1980, **21**, 143–152.
- 10 A. O. Ibhaddon, *J. Appl. Polym. Sci.*, 1992, **46**, 2123–2129.
- 11 Y. Liu, W. Li, L. Hou and P. Wu, *RSC Adv.*, 2014, **4**, 24263.